Paradoxical effects of increased expression of PGC-1α on muscle mitochondrial function and insulin-stimulated muscle glucose metabolism

Cheol Soo Choi[a,b,1], Douglas E. Befroy[a,1], Roberto Codella[a,1], Sheene Kim[a], Richard M. Reznick[a], Yu-Jin Hwang[a], Zhen-Xiang Liu[a], Hui-Young Lee[a], Alberto Distefano[a], Varman T. Samuel[a], Dongyan Zhang[a], Gary W. Cline[a], Christoph Handschin[c], Jiandie Lin[c], Kitt F. Petersen[a], Bruce M. Spiegelman[c], and Gerald I. Shulman[a,d,e,2]

Departments of [a]Internal Medicine and [d]Cellular and Molecular Physiology, and [e]Howard Hughes Medical Institute, Yale University School of Medicine, New Haven, CT 06510; [c]Department of Cell Biology, Dana–Farber Cancer Institute, Harvard Medical School, Boston, MA 02115; and [b]Lee Gil Ya Cancer and Diabetes Institute, Gachon University of Medicine and Science, Incheon 406-840, Korea

Contributed by Gerald I. Shulman, October 15, 2008 (sent for review August 21, 2008)

Peroxisome proliferator-activated receptor-γ coactivator (PGC)-1α has been shown to play critical roles in regulating mitochondria biogenesis, respiration, and muscle oxidative phenotype. Furthermore, reductions in the expression of PGC-1α in muscle have been implicated in the pathogenesis of type 2 diabetes. To determine the effect of increased muscle-specific PGC-1α expression on muscle mitochondrial function and glucose and lipid metabolism in vivo, we examined body composition, energy balance, and liver and muscle insulin sensitivity by hyperinsulinemic-euglycemic clamp studies and muscle energetics by using ^{31}P magnetic resonance spectroscopy in transgenic mice. Increased expression of PGC-1α in muscle resulted in a 2.4-fold increase in mitochondrial density, which was associated with an ≈60% increase in the unidirectional rate of ATP synthesis. Surprisingly, there was no effect of increased muscle PGC-1α expression on whole-body energy expenditure, and PGC-1α transgenic mice were more prone to fat-induced insulin resistance because of decreased insulin-stimulated muscle glucose uptake. The reduced insulin-stimulated muscle glucose uptake could most likely be attributed to a relative increase in fatty acid delivery/triglyceride reesterfication, as reflected by increased expression of CD36, acyl-CoA:diacylglycerol acyltransferase1, and mitochondrial acyl-CoA:glycerol-*sn*-3-phosphate acyltransferase, that may have exceeded mitochondrial fatty acid oxidation, resulting in increased intracellular lipid accumulation and an increase in the membrane to cytosol diacylglycerol content. This, in turn, caused activation of PKCθ, decreased insulin signaling at the level of insulin receptor substrate-1 (IRS-1) tyrosine phosphorylation, and skeletal muscle insulin resistance.

diacylglycerol | fatty acid oxidation | insulin resistance | magnetic resonance spectroscopy | mitochondria

Type 2 diabetes is the most common metabolic disease in the world, and although the primary cause of this disease is unknown, it is clear that insulin resistance plays an early and critical role in its pathogenesis (1–3). Many studies suggest that net lipid accumulation (4–6), caused by an imbalance between fatty acid delivery/synthesis and fatty acid oxidation, results in activation of a serine kinase cascade. This, in turn, inhibits insulin signaling, resulting in insulin resistance in liver and skeletal muscle, the organs responsible for the majority of glucose disposal. Studies in transgenic (TG) and knockout mice have demonstrated that alterations in fatty acid delivery (5, 7), synthesis (8), or mitochondrial (9–11)/peroxisomal (12) fatty acid oxidation can alter this balance, resulting in insulin resistance when there is a net increase in intracellular diacylglycerol content and protection from insulin resistance when there is a net reduction in intracellular diacylglycerol content.

Peroxisome proliferator-activated receptor-γ coactivator (PGC)-1α is a critical regulator of mitochondrial biogenesis in skeletal muscle and promotes this process in response to exercise to maintain a balance between energy need and energy supply (13, 14). Furthermore, 2 recent microarray studies have implicated decreased PGC-1α expression and reduction in the expression of OXPHOS genes encoded by PGC-1α in the pathogenesis of type 2 diabetes mellitus (15, 16). Therefore, we hypothesized that increased expression of PGC-1α would prevent against fat-induced insulin resistance. Given the important role of PGC-1α in stimulating mitochondrial biogenesis and potentially affecting the balance between fatty acid delivery/synthesis versus fatty acid oxidation in muscle, we decided to examine the impact of increased PGC-1α expression on in vivo muscle mitochondrial function and glucose and lipid metabolism in muscle-specific PGC-1α TG mice fed a high-fat diet.

Results

Increased Expression of PGC-1α in Muscle Elevated Mitochondrial Density and OXPHOS Genes. MCK-PGC-1α TG (MPGC-1α TG) mice had an ≈6-fold increase in gene expression of PGC-1α (Fig. 1*A*) and 2.4-fold higher mitochondrial density in the extensor digitorum longus muscle (EDL; mainly type II fibers), assessed by electron microscopy, as compared with WT mice (Fig. 1*B*). The expression of a number of OXPHOS and mitochondrial genes was significantly increased, including subunits of NADH-ubiquinone oxidoreductase (Ndufs1 and Ndufv2), cytochrome *c* (Cycs), cytochrome *c* oxidase (Cox5b), and ATP synthase (APT5o), which have been shown to be directly regulated by PGC-1α (Fig. 1*C*). However, there was no difference in mitochondrial density in soleus muscle (type I fiber muscle; data not shown), which indicates that increased expression of PGC-1α was predominant in type II fibers of MPGC-1α TG mice because of preferential expression of the MCK promoter in this fiber type.

Increased Expression of PGC-1α in Muscle Did Not Change Fat Mass or Energy Expenditure. Total body weight, fat mass, and lean body mass were similar between MPGC-1α TG and WT littermate mice fed a regular diet. High-fat feeding for 3 weeks increased fat mass in MPGC-1α TG mice to the same extent as in WT littermates (Table 1). To assess energy balance, mice were housed in metabolic cages for 4 days (2 days to acclimate followed by 2-day study). Consistent with the effects on body weight change, no differences in food

Author contributions: C.S.C., D.E.B., R.C., S.K., R.M.R., Y.-J.H., and G.I.S. designed research; C.S.C., D.E.B., R.C., S.K., R.M.R., Y.-J.H., Z.-X.L., H.-Y.L., A.D., and V.T.S. performed research; H.-Y.L., V.T.S., and C.H. contributed new reagents/analytic tools; C.S.C., D.E.B., R.C., S.K., R.M.R., Y.-J.H., Z.-X.L., A.D., V.T.S., D.Z., G.W.C., C.H., J.L., K.F.P., B.M.S., and G.I.S. analyzed data; and C.S.C., D.E.B., R.C., S.K., R.M.R., Y.-J.H., Z.-X.L., A.D., V.T.S., D.Z., G.W.C., C.H., J.L., K.F.P., B.M.S., and G.I.S. wrote the paper.

The authors declare no conflict of interest.

Freely available online through the PNAS open access option.

[1]C.S.C., D.E.B., and R.C. contributed equally to this work.

[2]To whom correspondence should be addressed. E-mail: gerald.shulman@yale.edu.

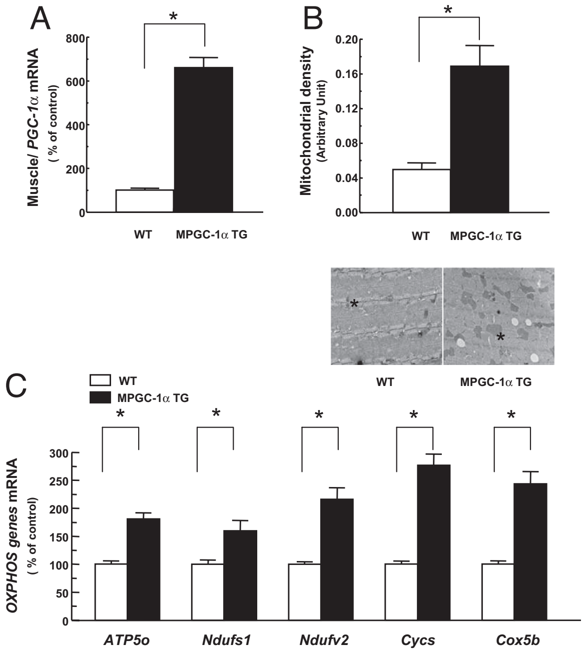

Fig. 1. Increased expression of PGC-1α in muscle elevated mitochondrial density and OXPHOS genes. Total RNA was isolated from tibialis anterior muscle of the mice fed a regular diet ($n = 5$). (*A* and *C*) PGC-1α (*A*) and OXPHOS genes (*C*) expression was assessed by real-time RT-PCR. (*B*) Mitochondrial density was counted in EDL muscle ($n = 5$). (Magnification: ×18,500.) The asterisk indicates mitochondrion. APT5o, ATP synthase; Ndufs, NADH-ubiquinone oxidoreductase; Cycs, cytochrome *c*; Cox5b, cytochrome *c* oxidase.

intake, activity, and total energy expenditure were observed between MPGC-1α TG and WT mice fed either regular chow or a high-fat diet (Table 1). The respiratory quotient (RQ), which represents substrate preference as fuel, indicated that whole-body fat oxidation was unaffected in MPGC-1α TG fed a regular chow [carbohydrate rich (12% fat)] diet. Switching WT mice to a high-fat diet (55% fat) significantly increased fat oxidation (reduced RQ) in the fed state, whereas altering the diet failed to increase fat oxidation any further in MPGC-1α TG mice. These data demonstrate that increased PGC-1α gene expression and mitochondrial density in skeletal muscle does not alter whole-body energy expenditure, body weight, or fat mass.

Insulin Sensitivity Was Paradoxically Decreased in MPGC-1α TG Mice Fed a High-Fat Diet. Fasting plasma glucose and insulin concentrations were similar between the 2 groups, fed either the regular or high-fat diet (Table 2). Plasma lipid profiles, including plasma fatty acids, triglycerides, and cholesterol, were similar under fasting and insulin-stimulated conditions in both groups fed either regular or high-fat diet (Table 2). No difference in insulin sensitivity, assessed by the hyperinsulinemic-euglycemic clamp, was observed in the 2 groups of mice when fed a regular diet (data not shown). In contrast, MPGC-1α TG mice were insulin-resistant compared with WT control mice when fed a high-fat diet, reflected by a 60% reduction in the glucose infusion rate required to maintain euglycemia during the clamp (Fig. 2*A*). The whole-body insulin resistance could be attributed mostly to a 25% reduction in insulin-stimulated whole-body glucose uptake and a 56% reduction in whole-body glycogen synthesis (Fig. 2*C*). There were no differences in basal or insulin-mediated suppression of hepatic glucose production between the groups (Fig. 2*B*). Consistent with the peripheral insulin resistance observed during the clamp, 2-deoxy glucose uptake was decreased by 60% in MPGC-1α TG mice compared with WT mice (Fig. 2*D*). These changes were associated with a reduction in insulin-stimulated IRS1 tyrosine phosphorylation and Akt2 activity (Fig. 2 *E* and *F*).

Mechanism for Increased Insulin Resistance in Skeletal Muscle in PGC-1α TG Mice. Consistent with our hypothesis of lipid metabolites inducing insulin resistance (6, 9, 10, 17–20), muscle triglyceride, lysophosphatidic acid, and long-chain acyl CoAs were markedly increased in MPGC-1α TG mice fed a high-fat diet compared with WT mice (Fig. 3 *A*, *C*, and *D*). The membrane/cytosol ratio of skeletal muscle diacylglycerol, a known activator of PKCs, was increased by ≈50% in the MPGC-1α TG mice compared with WT mice (Fig. 3*B*) and was associated with a 40% increase in PKCθ activity, as reflected by an increase in PKCθ translocation from cytosol to membrane (Fig. 3*E*).

A recent study suggested that PGC-1α induces insulin resistance in liver through peroxisome proliferator-activated receptor (PPAR)-α dependent induction of mammalian tribbles homolog (TRB-3), which has been suggested to be a direct negative regulator of AKT activity in some studies (21, 22), but not all (23, 24). Because overexpression of PGC-1α was also found to significantly increase TRB-3 expression in skeletal muscle (25) we examined TRB-3 gene expression in the muscle of MPGC-1α TG mice. TRB-3 mRNA and protein levels were ≈2-fold increased in MPGC-1α TG mice compared with WT mice (Fig. 4).

Muscle Oxidative Function In Vivo and Ex Vivo. Net intracellular lipid accumulation in skeletal muscle can occur as a result of increased fatty acid delivery/synthesis and/or reduced fatty acid oxidation. To estimate mitochondrial function in vivo we used ^{31}P saturation-transfer magnetic resonance spectroscopy (MRS) to assess the unidirectional rate of muscle ATP synthesis (V_{ATP}) (26, 27). Skeletal muscle V_{ATP} was increased by 50–60% in the hindlimb of MPGC-1α TG mice fed either regular or high-fat diet compared with the WT mice (Fig. 5 *A* and *B*). In addition, the ratio of inorganic phosphate to phosphocreatine was increased by 53% in MPGC-1α TG mice fed a high-fat diet compared with WT mice (0.236 ± 0.01 vs. 0.154 ± 0.01, $P < 0.001$), which may reflect a higher ratio of type I fibers (mostly oxidative) to type II fibers (mostly glycolytic) (28). Rates of fat oxidation measured ex vivo in isolated muscle strips were increased by 30% in the EDL (predom-

Table 1. Basal metabolic parameters of energy balance

Parameter	Regular diet: WT, $n = 8$	Regular diet: MPGC-1α TG, $n = 8$	High-fat diet: WT, $n = 8$	High-fat diet: MPGC-1α TG, $n = 8$
Body weight, g	28.6 ± 0.4	28.2 ± 0.8	32.4 ± 0.7	32.3 ± 0.8
Fat mass, g	1.91 ± 0.2	2.1 ± 0.3	5.64 ± 0.6	5.9 ± 0.5
Lean body mass, g	22.2 ± 0.4	21.7 ± 0.7	22.3 ± 0.2	22.3 ± 0.4
Total energy expenditure, kcal /h/kg body mass	16.0 ± 0.8	15.1 ± 0.8	16.5 ± 0.3	16.1 ± 0.9
Food intake, kcal /h/kg body mass	18.3 ± 1.5	15.5 ± 1.6	19.7 ± 2.3	18.1 ± 2.6
Activity, count/h	103.5 ± 26.3	111.0 ± 21.5	110.4 ± 19.7	81.1 ± 26.0
Respiratory quotient	0.929 ± 0.012	0.880 ± 0.023	0.840 ± 0.010	0.820 ± 0.010

Table 2. Plasma metabolite, hormone, and cytokine data from high-fat-fed WT and PGC-1α TG mice

	Regular diet				High-fat diet			
	Fast		Clamp		Fast		Clamp	
Measure	WT, $n = 9$	MPGC1α TG, $n = 9$	WT, $n = 9$	MPGC1α TG, $n = 9$	WT, $n = \approx$7–9	MPGC1α TG, $n = \approx$7–9	WT, $n = 9$	MPGC1α TG, $n = 6$
Glucose, mg/dL	150 ± 11	142 ± 9	118 ± 3	114 ± 4	160 ± 7	164 ± 10	123 ± 3	119 ± 5
Insulin, μU/mL	14.6 ± 1.7	13.4 ± 1.6	61.4 ± 5.8	63.1 ± 5.4	17.7 ± 1.6	20.3 ± 1.2	60.9 ± 5.2	73.3 ± 5.2
Fatty acids, mEq/L	0.98 ± 0.11	1.27 ± 0.13	0.58 ± 0.06	0.48 ± 0.09	0.98 ± 0.09	1.00 ± 0.04	0.90 ± 0.07	0.83 ± 0.06
Triglycerides, mg/dL					69.5 ± 9.1	83.2 ± 7.9	ND	ND
Cholesterol, mg/dL					91.1 ± 7.7	88.9 ± 2.5	ND	ND
β-Hydroxbutyrate, mM					1.47 ± 0.25	0.9 ± 0.10	ND	ND

ND, not determined.

inantly type IIb muscle fibers) of MPGC-1α TG mice compared with WT mice, but were unaltered in soleus muscle (mainly type I muscle fibers) (Fig. 5 *C* and *D*).

Gene Expression Involved in Fatty Acid Oxidation and Uptake. Consistent with effects on muscle oxidative function, the expression of the oxidative/thermogenic genes (*CPT1*, *CPT2*, *VLCAD*, *LCAD*, *MCAD*, and *UCP2*) and carnitine palmitoyl transferase 1 (CPT1) protein were increased in tibialis anterior muscle (predominantly type II muscle fibers) of MPGC-1α TG mice with respect to WT mice (Fig. 5 *E* and *F*). In addition, gene and protein expression of acetyl coenzyme A carboxylase 2 (ACC2) was increased and the phospho-ACC2 level was also increased in MPGC-1α TG mice compared with WT mice (Fig. 5 *E* and *F*). However, there was no difference in AMP-activated protein kinase (AMPK)-α2 activity in the EDL muscle between the 2 groups [WT ($n = 6$) vs. TG mice ($n = 6$): 0.63 ± 0.08 vs. 0.58 ± 0.18 pmol/min per mg, not significant]. There was a marked increase in the expression of genes of fatty acid transport (*CD36*) and fatty acid reesterification [mitochondrial acyl-CoA:glycerol-*sn*-3-phosphate acyltransferase (mtGPAT) and acyl-CoA:diacylglycerol acyltransferase1 (DGAT1)] in skeletal muscle of the MPGC-1α TG mice compared with the WT mice (Fig. 6).

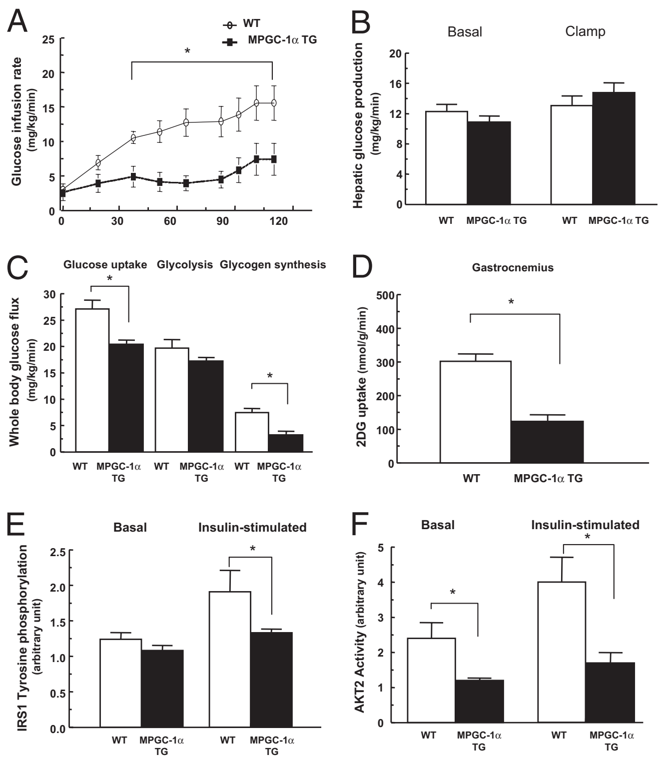

Fig. 2. Increased expression of PGC-1α in skeletal muscle paradoxically decreased peripheral insulin sensitivity in high-fat fed mice. (*A–D*) Peripheral and hepatic insulin sensitivity was assessed by hyperinsulinemic-euglycemic clamps. (*A*) Glucose infusion rates. (*B*) Hepatic glucose production. (*C*) Whole-body glucose uptake, glycolysis, and glycogen synthesis. (*D*) skeletal muscle (gastrocnemius) glucose uptake. (*E* and *F*) Consistent with decreased muscle insulin sensitivity, IRS1 tyrosine phosphorylation and AKT2 activity in skeletal muscle (gastrocnemius) were decreased in MPGC-1α TG compared with WT mice. IRS1 tyrosine phosphorylation and Akt2 activity were assessed 14 min after i.p. insulin injection of 1 unit/kg body weight. $n = 6–8$ per group.

Discussion

Given the important role that muscle mitochondria play in whole-body glucose and fat metabolism we sought to examine the impact of increased mitochondrial content on oxidative metabolism and fat-induced insulin resistance in TG mice with increased expression of PGC-1α in skeletal muscle. We found that the increased mitochondrial content in these TG mice was accompanied by increased oxidative metabolism measured both in vivo and ex vivo; however, that did not prevent diet-induced obesity. Furthermore, MPGC-1α TG mice were more prone to fat-induced muscle insulin resistance, which could be attributed to reduced insulin-stimulated glucose uptake in skeletal muscle.

These results are contrary to previous studies that found increased glucose uptake in both C2C12 and L6 muscle cells that overexpressed PGC-1α (29) and ex vivo muscle with electrotransfection of PGC-1α (30). It is possible that the differences in these results may be caused by the relatively higher expression of PGC-1α in the TG mice compared with the in vitro studies. However, it should be noted that the increased expression of PGC-1α in muscles composed of type II fibers was $\approx$6-fold, which is well within the 10- to 13-fold increase observed after exercise training and similar to that found in type I muscle fibers (31). Moreover, in contrast to the current in vivo studies, insulin sensitivity under conditions of increased fatty acid exposure was not tested in these in vitro-cultured cell and ex vivo muscle studies (29, 30).

To understand the mechanism for the reduced insulin-stimulated glucose uptake in skeletal muscle in the MPGC-1α TG mice we examined the insulin signaling pathway and found that both insulin-stimulated IRS-1 tyrosine phosphorylation and insulin-stimulated AKT2 activity were significantly reduced in skeletal muscle. In addition, we found that the expression of TRB-3, a mammalian homolog of *Drosophila* tribble, which has recently been suggested by some studies (21, 22), but not all (23, 24), to be a direct negative regulator of AKT activity, was increased by $\approx$2-fold in skeletal muscle of the PGC-1α TG mice, consistent with previous observations (25). However, given the controversy regarding the role of TRB-3 in causing insulin resistance, further studies will be necessary to determine whether increased TRB-3 expression contributes to the observed insulin resistance in MPGC-1α TG mice. Furthermore, because TRB-3 has been implicated to cause insulin resis-

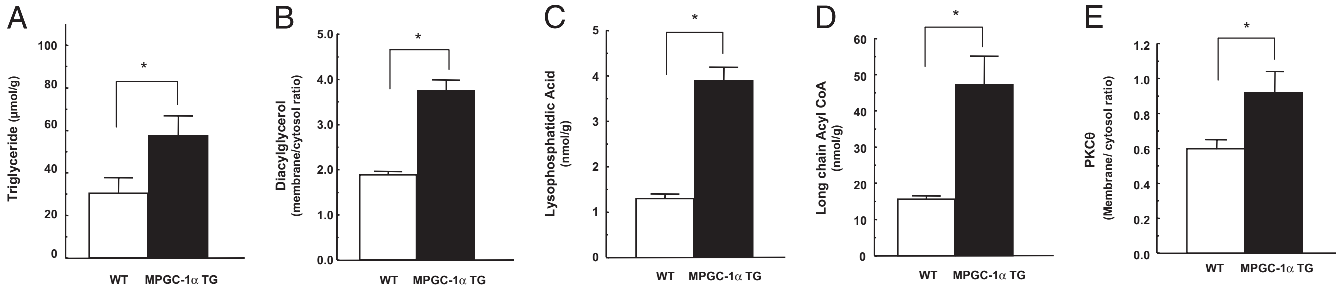

Fig. 3. Fat metabolites and membrane translocation of PKCθ were increased in skeletal muscle of MPGC-1α TG mice. (*A*, *C*, and *D*) Triglyceride (*A*), lysophosphatidic acid (*C*), and long-chain acyl-CoA (*D*) levels were significantly increased in muscle (gastrocnemius) in MPGC-1α TG mice. (*B* and *E*) Membrane/cytosol ratio of diacylglycerol (*B*) and PKCθ (*E*) were significantly higher in muscle (gastrocnemius) of MPGC-1α TG mice compared with WT mice. $n = 8$ per group.

tance at the level of AKT2 it cannot explain the reduced insulin-stimulated IRS-1 tyrosine phosphorylation. Previous studies have implicated that increases in intracellular diacylglycerol, caused by an imbalance between fatty acid delivery/synthesis and fatty acid oxidation, results in activation of PKCθ, which reduces insulin signaling at the level of the insulin receptor and IRS-1 tyrosine phosphorylation in muscle (6, 17). Consistent with this hypothesis, we observed increases in membrane/cytosol ratio of diacylglycerol, associated with increased activation of PKCθ in the MPGC-1α TG mice.

This result was unexpected given the 2-fold increase in mitochondrial content. To determine whether the mitochondria were dysfunctional, we examined a biomarker of in vivo mitochondrial function in the MPGC-1α TG mice with ^{31}P saturation-transfer MRS (32). Using this approach we found that mitochondrial ATP synthesis per g of muscle was increased by 60% in the MPGC-1α TG mice, which was somewhat less than the 2.4-fold increase in mitochondrial density, suggesting partial down-regulation of activity per unit of mitochondrial mass in the MPGC-1α TG mice. However, the mechanism responsible for this effect remains to be determined. Despite increased muscle ATP production in vivo, and enhanced fat oxidation ex vivo, in MPGC-1α TG mice, no effects on whole-body energy expenditure could be detected. Potentially, these mice could have enhanced mitochondrial coupling of oxidative phosphorylation (an elevated P/O ratio). We have estimated the efficiency of mitochondrial energy production in vivo in a variety of human and animal models by using MRS biomarkers of mitochondrial metabolism and have found that the P/O ratio is unaffected (32, 33) unless mitochondrial coupling is deliberately targeted (e.g., by T_3/2,4-dinitrophenol treatment) or uncoupling

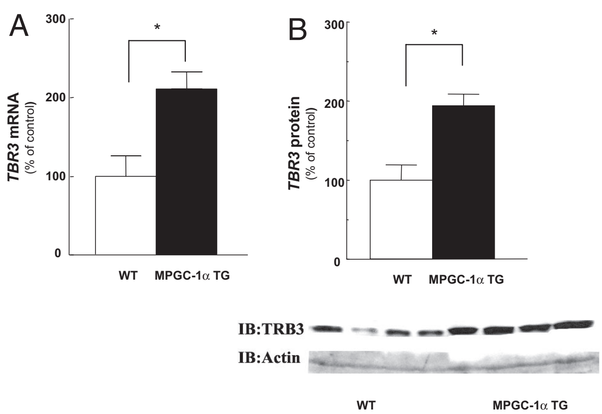

Fig. 4. Increased expression of PGC-1α in muscle also elevated TRB-3 gene ($n = 8$) and protein expression ($n = 4$) in skeletal muscle. Total RNA was isolated from tibialis anterior muscle, TRB-3 gene expression was assessed by real-time RT-PCR (*A*), and protein expression was confirmed by immunoblot (*B*).

protein expression is modulated (26, 34, 35). More recently, we have observed that endurance trained human muscle, likely to have an increased mitochondrial content, is actually less well coupled under resting conditions (27). Therefore, we believe that modulation of the P/O ratio is unlikely to cause the effects observed in these mice. A more likely explanation is that the measurement of whole-body energy expenditure is not sensitive enough to detect an increase in muscle ATP production.

Given the significant increase in intramuscular triglyceride and fat metabolites in the MPGC-1α TG mice, despite a concomitant increase in mitochondrial function and fatty acid oxidation, we investigated whether this could be attributed to increased fatty acid delivery and/or fat synthesis in the skeletal muscle of these mice. Consistent with this hypothesis, we found that gene expression for *CD36*, a key fatty acid transporter, and *mtGPAT and DGAT1*, 2 key rate-controlling enzymes for triglyceride reesterification, were markedly increased in the muscle of the MPGC-1α TG mice. It has been demonstrated that PGC-1α coactivates PPARs and the promoter of CD36 has a PPAR response element sequence (36); therefore, increased expression of PGC-1α could result in enhanced CD36 expression and increased uptake of fatty acids. However, the mechanism by which increased PGC-1α expression elevates the gene expression of *mtGPAT* and *DGAT1* is less clear. PGC-1α, in contrast to PGC-1β, is not known to regulate sterol-regulatory element binding protein 1c activity (37), although it is possible that interactions via liver X receptor could affect these genes (37, 38).

Taken together, these data are consistent with the hypothesis that under normal physiologic conditions of exercise PGC-1α induces a coordinated program of increased energy delivery and increased mitochondrial biogenesis and fatty acid oxidation to meet the increased energy demands of working skeletal muscle. In contrast, this same coordinated program, in the nonexercising MPGC-1α TG mice, results in a mismatch between increased fatty acid uptake and that of mitochondrial fat oxidation, resulting in a net increase of intramyocellular fat and diacylglycerol content and insulin resistance. Recently, Koves *et al.* (39) proposed that fat-induced insulin resistance in muscle might also arise from increased fatty acid transport into mitochondria, resulting in incomplete β-oxidation. Further studies will be necessary to determine whether this mechanism also contributes to skeletal muscle insulin resistance in this mouse model.

In summary, we have shown that increased muscle expression of PGC-1α paradoxically exacerbated fat-induced insulin resistance in skeletal muscle despite an increase in mitochondrial density and mitochondrial activity. This insulin resistance could be attributed to net increases in the membrane/cytosol diacylglycerol content, caused by relative increases in fatty acid uptake and reesterification exceeding mitochondrial fatty acid oxidation. The increase in membrane/cytosol diacylglycerol content, in turn, leads to activation of PKCθ and decreased insulin signaling at the level of IRS-1

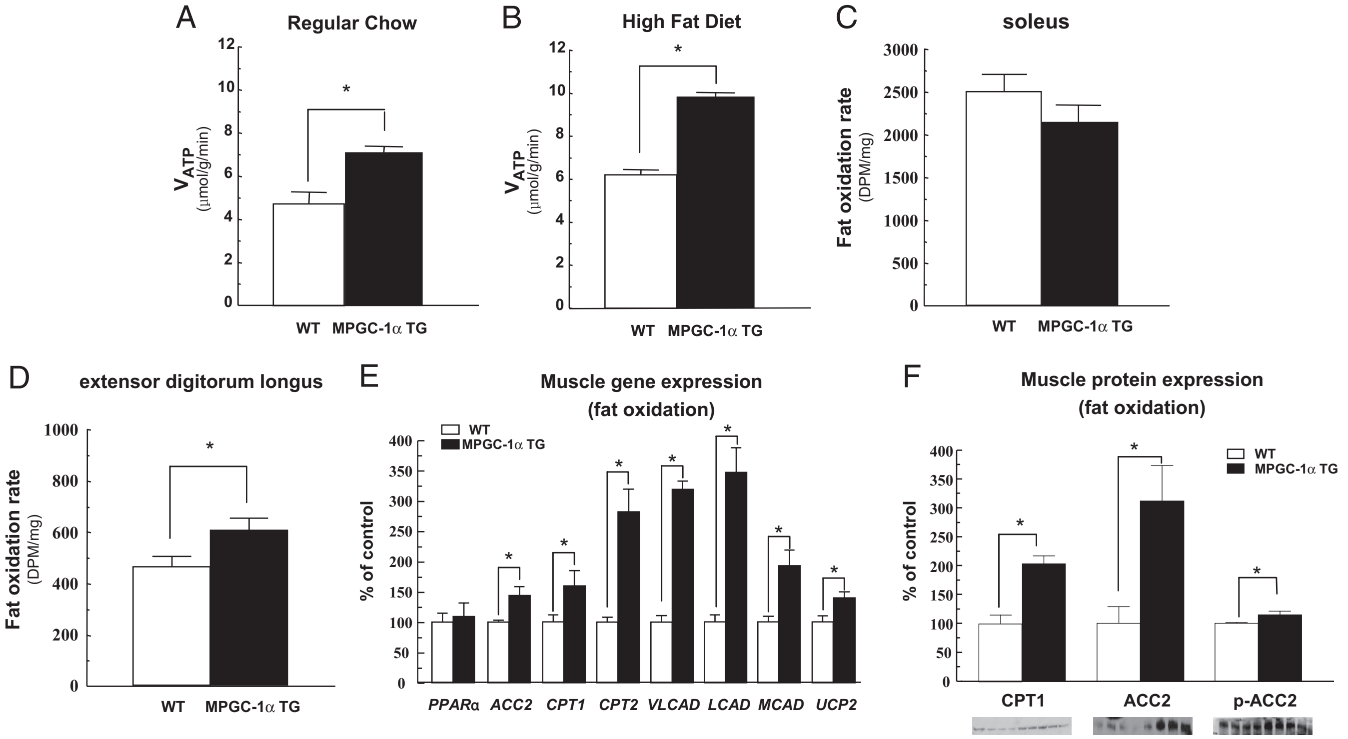

Fig. 5. In vivo rates of ATP production and ex vivo fat oxidation were increased in the muscle of increased PGC-1α expression. (*A* and *B*) Saturation transfer measurements of ATP synthesis rates (V_{ATP}) by ^{31}P-MRS in hind limb of mice (n = 6) on regular chow (*A*) and high-fat diet (*B*). (*C* and *D*) Ex vivo skeletal muscle fat oxidation rate in soleus muscle (*C*) and EDL muscle (*D*) from mice (n = 6) fed regular chow. (*E*) The expression of oxidative/thermogenic genes in tibialis anterior muscle from mice (n = 5–6) fed regular chow assessed by real-time RT-PCR. (*F*) Immunoblot analysis (n = 4) from selected genes for CPT1, ACC2, and phospho-ACC2 (Ser-219/221). VLCAD, very long-chain acyl-CoA dehydrogenase; LCAD, long-chain acyl-CoA dehydrogenase; MCAD, medium-chain acyl-CoA dehydrogenase; UCP2, uncoupling protein 2.

tyrosine phosphorylation and results in insulin resistance in skeletal muscle.

Materials and Methods

Animals. MPGC-1α TG mice were generated as described (40). PGC-1α complementary DNA was placed downstream of a 6.5-kb MCK promoter sequence. MPGC-1α TG mice were generated by standard DNA microinjection and identified by PCR-based genotyping. Male MPGC-1α TG mice and littermates (12–14 weeks of age) were studied under controlled temperature (22 ± 2 °C) and lighting (12-h light, 0700–1700 h; 12-h dark, 1700–0700 h). To examine diet-induced changes in glucose and fat metabolism, male MPGC-1α TG and WT mice were fed a high-fat diet (55% fat by calories; Harlan Teklad) ad libitum for 3 weeks. All mice were maintained in accordance with the Institutional Animal Care and Use Committee of Yale University School of Medicine.

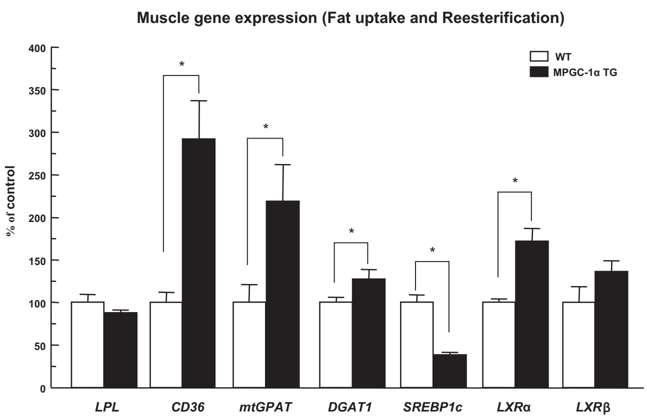

Fig. 6. The expression of the genes involved in fatty acid uptake and reesterification was increased in tibialis anterior muscle of MPGC-1α TG mice fed regular chow (n = 5–6).

Basal Metabolic Parameters. Fat and lean body masses were assessed by a ^{1}H minispec system (Bruker BioSpin) before and after 3 weeks of high-fat feeding. Activity, food consumption, and energy expenditure were evaluated before and after 3 weeks of high-fat feeding (CLAMS; Columbus Instruments) as described (10).

Hyperinsulinemic-Euglycemic Clamp Study. After an overnight fast, a hyperinsulinemic-euglycemic clamp was conducted for 120 min with a primed/continuous infusion of human insulin (126 pmol/kg prime, 18 pmol/kg per min infusion) (Novo Nordisk) as described (10). During the clamp, plasma glucose was maintained at basal concentrations (≈6.7 mM). Rates of basal and insulin-stimulated whole-body glucose fluxes and tissue glucose uptake were determined as described (10).

Biochemical Analysis. Plasma glucose and insulin were determined by a glucose oxidase method (Beckman glucose analyzer II) and RIA (RIA kit from Linco Research). Plasma FFA was determined by using an acyl-CoA oxidase based colorimetric kit (Wako Pure Chemical Industries). Plasma resistin, leptin, TNF-α, and IL-6 were measured by multiplexed biomarker immunoassays (Lincoplex) from Linco Research.

Insulin Signaling and PKCθ. IRS1 tyrosine phosphorylation and Akt2 activity were assessed in protein extracts from muscle harvested after short-term insulin stimulation as described (10). Primary antibodies used for experiments were rabbit polyclonal IgG. Antibodies for IRS1 tyrosine phosphorylation and Akt2 were obtained from Upstate. PKCθ membrane translocation assay was conducted as described (10). Membrane translocation of PKCθ was expressed as the ratio of membrane bands over cytosol bands (arbitrary units).

Total RNA Preparation, Real-Time Quantitative RT-PCR Analysis, and Immunoblotting Analysis. Total RNA was isolated from tibialis anterior muscle of the mice fed regular diet by using total RNA isolation reagent (BL-10500; Biotecx Laboratories). Quantitative RT-PCR was performed with custom-made RT-PCR enzymes and a reagents kit (Invitrogen Life Technology) and an ABI Prism 7700 Sequence

Detector (PE Applied Biosciences). For Western protein analysis, 40 μg of cell lysates was then separated on 4–12% SDS/PAGE and immunoblotted with TRB-3 antibody (provided by Marc Montminy, Peptide Biology Laboratories, Salk Institute for Biological Studies, La Jolla, CA). CPT1 (Santa Cruz Biotechnology), ACC2 (Santa Cruz Biotechnology), or anti-p-ACC 2 (Ser-219/221; Santa Cruz Biotechnology) antibodies.

AMPK Activity Assays. The EDL muscle was quickly freeze-clamped in situ and kept in liquid nitrogen until analyzed. AMPK activity was assessed as described (41). Muscles were ground and mixed with 1 mL of lysis buffer. Homogenates were spun at 20,800 $\times$ g for 10 min at 4 °C, and protein concentrations were determined. AMPK-α_2 was immunoprecipitated overnight from cell lysates containing 1 mg of protein by using 1 μL of AMPK-α_2 antibody (Santa Cruz Biotechnology). Skeletal muscle AMPK-α_2 activity was determined by after the incorporation of [^{32}P]ATP into a synthetic peptide containing the AMARA sequence the next day.

Transmission Electron Microscopy Analysis. Mitochondrial densitiy was assessed by a Tecnai 12 BiolTWIN electron microscope (FEI) in soleus and EDL muscle as described (18). For each set of 5 pictures from 3 random sections of individual muscle, average volume density was calculated and the mean of 3 values was used to estimate the volume density for each muscle.

Tissue Lipid Measurement. Intracellular fatty acid metabolites, such as lysophosphatidic acid, and long-chain fatty acyl-CoAs were measured by using an API 4000 tandem mass spectrometer (Applied Biosystems) in conjunction with 2 PerkinElmer 200 Series micro pumps and a 200 Series autosampler (PerkinElmer) (8). To determine the level of diacylglycerol in cytosol and membrane, diacylglycerol extraction and analysis in both cytosolic and membrane samples was performed as described (8, 19). Tissue triglyceride was extracted by using the method of Bligh and Dyer (42) and measured by using a DCL Triglyceride Reagent (Diagnostic Chemicals).

Skeletal Muscle Fatty Acid Oxidation Rate. Skeletal muscle ($\approx$10–15 mg of soleus and EDL muscles) were quickly removed from mice, and muscle fatty acid oxidation was assessed with trapping $^{14}CO_2$ after incubation with albumin-bound 2 μCi of [1-^{14}C] oleic acid (43).

Unidirectional Rate of Muscle ATP Synthesis by In Vivo ^{31}P-MRS. The unidirectional rate of muscle ATP synthesis (V_{ATP}) was assessed by ^{31}P saturation-transfer MRS using a 9.4 T superconducting magnet (Magnex Scientific) interfaced to a Bruker Biospec console. After an overnight fast, the mouse was sedated by using $\approx$1% isoflurane, and the left hindlimb was positioned under a 15-mm-diameter ^{31}P surface coil. Nonlocalized ^{31}P saturation-transfer spectra were acquired with saturation of the γ-ATP resonance or at a downfield frequency equidistant from the Pi resonance (control saturation) using the following parameters: 1-ms AHP excitation pulse (centered between Pi and γ-ATP), 10-s frequency-selective saturation pulse, sweep width 8 kHz, 1,024 complex points, effective T_R 10 s, 64 averages. Fully-relaxed ^{31}P spectra (T_R 25 s, 32 averages) were also obtained to determine metabolite concentrations. The T_1 of P_i under γ-ATP saturation (T_1') was measured by using an 8-point inversion-recovery sequence (2-ms AFP inversion pulse) with γ-ATP-saturation before and during the inversion delay. All MR data were processed with XWINNMR (version 6.5; Bruker Biospin); before Fourier transformation ^{31}P free induction decays were zero-filled to 32k points and multiplied by a mixed Lorentzian/Gaussian function (lb −20/ gb 0.04). ^{31}P spectra were baseline corrected by fitting to a fifth-order polynomial. The unidirectional rate of $P_i \rightarrow$ ATP flux was determined as described (26, 27).

Statistics. All results are expressed as means $\pm$ SEM of n observations. Statistical differences between the means were assessed by a 2-tailed Student's t test; *, $P < 0.05$.

ACKNOWLEDGMENTS. We thank Mario Kahn and Xiaoxian Ma for expert technical assistance. This work was supported by U.S. Public Health Services Grants R01 DK-40936, U24 DK-76169, and P30 DK-45735 (to G.I.S.). G.I.S. is an Investigator of The Howard Hughes Medical Institute and the recipient of a Distinguished Clinical Investigator Award from the American Diabetes Association.

1. Zimmet P, Alberti KG, Shaw J (2001) Global and societal implications of the diabetes epidemic. *Nature* 414:782–787.
2. Lillioja S, *et al.* (1993) Insulin resistance and insulin secretory dysfunction as precursors of non-insulin-dependent diabetes mellitus: Prospective studies of Pima Indians. *N Engl J Med* 329:1988–1992.
3. DeFronzo RA, Bonadonna RC, Ferrannini E (1992) Pathogenesis of NIDDM: A balanced overview. *Diabetes Care* 15:318–368.
4. Boden G, Shulman GI (2002) Free fatty acids in obesity and type 2 diabetes: Defining their role in the development of insulin resistance and β-cell dysfunction. *Eur J Clin Invest* 32(Suppl 3):14–23.
5. Kim JK, *et al.* (2001) Tissue-specific overexpression of lipoprotein lipase causes tissue-specific insulin resistance. *Proc Natl Acad Sci USA* 98:7522–7527.
6. Shulman GI (2000) Cellular mechanisms of insulin resistance. *J Clin Invest* 106:171–176.
7. Kim JK, *et al.* (2004) Inactivation of fatty acid transport protein 1 prevents fat-induced insulin resistance in skeletal muscle. *J Clin Invest* 113:756–763.
8. Neschen S, *et al.* (2005) Prevention of hepatic steatosis and hepatic insulin resistance in mitochondrial acyl-CoA:glycerol-sn-3-phosphate acyltransferase 1 knockout mice. *Cell Metab* 2:55–65.
9. Choi CS, *et al.* (2007) Overexpression of uncoupling protein 3 in skeletal muscle protects against fat-induced insulin resistance. *J Clin Invest* 117:1995–2003.
10. Choi CS, *et al.* (2007) Continuous fat oxidation in acetyl-CoA carboxylase 2 knockout mice increases total energy expenditure, reduces fat mass, and improves insulin sensitivity. *Proc Natl Acad Sci USA* 104:16480–16485.
11. Zhang D, *et al.* (2007) Mitochondrial dysfunction due to long-chain Acyl-CoA dehydrogenase deficiency causes hepatic steatosis and hepatic insulin resistance. *Proc Natl Acad Sci USA* 104:17075–17080.
12. Neschen S, *et al.* (2007) n-3 Fatty acids preserve insulin sensitivity in vivo in a peroxisome proliferator-activated receptor-α-dependent manner. *Diabetes* 56:1034–1041.
13. Puigserver P, *et al.* (1999) Activation of PPARγ coactivator-1 through transcription factor docking. *Science* 286:1368–1371.
14. Wu Z, *et al.* (1999) Mechanisms controlling mitochondrial biogenesis and respiration through the thermogenic coactivator PGC-1. *Cell* 98:115–124.
15. Mootha VK, *et al.* (2003) PGC-1α-responsive genes involved in oxidative phosphorylation are coordinately down-regulated in human diabetes. *Nat Genet* 34:267–273.
16. Patti ME, *et al.* (2003) Coordinated reduction of genes of oxidative metabolism in humans with insulin resistance and diabetes: Potential role of PGC1 and NRF1. *Proc Natl Acad Sci USA* 100:8466–8471.
17. Griffin ME, *et al.* (1999) Free fatty acid-induced insulin resistance is associated with activation of protein kinase C θ and alterations in the insulin signaling cascade. *Diabetes* 48:1270–1274.
18. Morino K, *et al.* (2005) Reduced mitochondrial density and increased IRS-1 serine phosphorylation in muscle of insulin-resistant offspring of type 2 diabetic parents. *J Clin Invest* 115:3587–3593.
19. Yu C, *et al.* (2002) Mechanism by which fatty acids inhibit insulin activation of insulin receptor substrate-1 (IRS-1)-associated phosphatidylinositol 3-kinase activity in muscle. *J Biol Chem* 277:50230–50236.
20. Kim JK, *et al.* (2004) PKC-θ knockout mice are protected from fat-induced insulin resistance. *J Clin Invest* 114:823–827.
21. Du K, Herzig S, Kulkarni RN, Montminy M (2003) TRB3: A tribbles homolog that inhibits Akt/PKB activation by insulin in liver. *Science* 300:1574–1577.
22. Koo SH, *et al.* (2004) PGC-1 promotes insulin resistance in liver through PPAR-α-dependent induction of TRB-3. *Nat Med* 10:530–534.
23. Iynedjian PB (2005) Lack of evidence for a role of TRB3/NIPK as an inhibitor of PKB-mediated insulin signalling in primary hepatocytes. *Biochem J* 386:113–118.
24. Okamoto H, *et al.* (2007) Genetic deletion of Trb3, the mammalian *Drosophila* tribbles homolog, displays normal hepatic insulin signaling and glucose homeostasis. *Diabetes* 56:1350–1356.
25. Mortensen OH, Frandsen L, Schjerling P, Nishimura E, Grunnet N (2006) PGC-1α and PGC-1β have both similar and distinct effects on myofiber switching toward an oxidative phenotype. *Am J Physiol* 291:E807–E816.
26. Jucker BM, *et al.* (2000) Assessment of mitochondrial energy coupling in vivo by 13C/31P NMR. *Proc Natl Acad Sci USA* 97:6880–6884.
27. Befroy DE, *et al.* (2008) Increased substrate oxidation and mitochondrial uncoupling in skeletal muscle of endurance trained individuals. *Proc Natl Acad Sci USA* 105:16701–16706.
28. Kushmerick MJ, Moerland TS, Wiseman RW (1992) Mammalian skeletal muscle fibers distinguished by contents of phosphocreatine, ATP, and Pi. *Proc Natl Acad Sci USA* 89:7521–7525.
29. Michael LF, *et al.* (2001) Restoration of insulin-sensitive glucose transporter (GLUT4) gene expression in muscle cells by the transcriptional coactivator PGC-1. *Proc Natl Acad Sci USA* 98:3820–3825.
30. Benton CR, *et al.* (2007) Modest PGC-1α overexpression in muscle in vivo is sufficient to increase insulin sensitivity and palmitate oxidation in SS, not IMF, mitochondria. *J Biol Chem* 283:4228–4240.
31. Miura S, Kai Y, Ono M, Ezaki O (2003) Overexpression of peroxisome proliferator-activated receptor γ coactivator-1α down-regulates GLUT4 mRNA in skeletal muscles. *J Biol Chem* 278:31385–31390.
32. Petersen KF, *et al.* (2003) Mitochondrial dysfunction in the elderly: Possible role in insulin resistance. *Science* 300:1140–1142.
33. Befroy DE, *et al.* (2007) Impaired mitochondrial substrate oxidation in muscle of insulin-resistant offspring of type 2 diabetic patients. *Diabetes* 56:1376–1381.
34. Lebon V, *et al.* (2001) Effect of triiodothyronine on mitochondrial energy coupling in human skeletal muscle. *J Clin Invest* 108:733–737.
35. Cline GW, *et al.* (2001) In vivo effects of uncoupling protein-3 gene disruption on mitochondrial energy metabolism. *J Biol Chem* 276:20240–20244.
36. Teboul L, *et al.* (2001) Structural and functional characterization of the mouse fatty acid translocase promoter: Activation during adipose differentiation. *Biochem J* 360:305–312.
37. Lin J, *et al.* (2005) Hyperlipidemic effects of dietary saturated fats mediated through PGC-1β coactivation of SREBP. *Cell* 120:261–273.
38. Oberkofler H, Schraml E, Krempler F, Patsch W (2003) Potentiation of liver X receptor transcriptional activity by peroxisome-proliferator-activated receptor γ coactivator 1 α. *Biochem J* 371:89–96.
39. Koves TR, *et al.* (2008) Mitochondrial overload and incomplete fatty acid oxidation contribute to skeletal muscle insulin resistance. *Cell Metab* 7:45–56.
40. Lin J, *et al.* (2002) Transcriptional coactivator PGC-1α drives the formation of slow-twitch muscle fibers. *Nature* 418:797–801.
41. Reznick RM, *et al.* (2007) Aging-associated reductions in AMP-activated protein kinase activity and mitochondrial biogenesis. *Cell Metab* 5:151–156.
42. Bligh EG, Dyer WJ (1959) A rapid method of total lipid extraction and purification. *Can J Biochem Physiol* 37:911–917.
43. Cha SH, Hu Z, Chohnan S, Lane MD (2005) Inhibition of hypothalamic fatty acid synthase triggers rapid activation of fatty acid oxidation in skeletal muscle. *Proc Natl Acad Sci USA* 102:14557–14562.